

Theory of Stereomutation Dynamics and Parity Violation in Hydrogen Thioperoxide Isotopomers $^{1,2,3}\text{HSO}^{1,2,3}\text{H}$

by Martin Quack* and Martin Willeke

Physical Chemistry, ETH Zürich, CH-8093 Zürich
(phone: ++41 1 632 44 21, fax: ++41 1 632 10 21, e-mail: Martin@Quack.ch)

Dedicated to Jack D. Dunitz on the occasion of his 80th birthday

We present quantitative calculations of the mode-selective stereomutation tunneling and parity violation in chiral hydrogen thioperoxide ('oxadisulfane') isotopomers XSOY with X, Y = H, D, and T. The torsional tunneling stereomutation dynamics are investigated with a quasi-adiabatic channel quasi-harmonic reaction path Hamiltonian approach, which treats the torsional motion anharmonically in detail and all remaining coordinates as harmonic (but anharmonically coupled to the reaction coordinate). We predict how stereomutation is catalyzed or inhibited by excitation of various vibrational modes compared to the corresponding stereomutation dynamics of the vibrational ground state. Parity-violating potentials were calculated with our recent multiconfiguration linear response (MC-LR) approach in the random phase approximation (RPA). We find that, in agreement with general scaling expectations, the parity-violating energy difference for the equilibrium structures of the two HSOH enantiomers (*ca.* 5×10^{-12} J mol⁻¹) is situated intermediate between HOOH and HSSH. Our results on the stereomutation dynamics and the influence of parity violation on these are discussed in relation to investigations for the analogous molecules H₂O₂, H₂S₂, and Cl₂S₂. As expected in XSOY (X, Y = H, D, and T), this influence is much larger than in the corresponding H₂O₂ isotopomers, but smaller than in H₂S₂ or Cl₂S₂.

1. Introduction. – Helical chirality has found fundamental interest in various contexts, in particular also with chiral biopolymers [1], where it is usually found in combination with the more-ordinary chirality of organic chemistry arising from the asymmetrically substituted C-atom. However, helical chirality arises also in some of the simplest examples for molecular chirality. Dihydrogendichalcogenides HXYH and related compounds are such examples, which show chirality by C₂ or C₁ (X ≠ Y) symmetry of their equilibrium geometry. They are relevant not only for atmospheric chemistry but also from a theoretical point of view. They are among the simplest prototypes of stereomutation dynamics after mode-selective excitation and, in particular, for the interaction between large-amplitude internal rotation (the torsion around the X–Y bond) with high-frequency HX or HY stretching dynamics. The barrier heights for stereomutation show wide variation for these and related compounds, for example $V_{\text{el,trans}}(\text{H}_2\text{O}_2) \approx 366 \text{ cm}^{-1}$ [2] but $V_{\text{el,trans}}(\text{H}_2\text{S}_2) \approx 2148 \text{ cm}^{-1}$ [3] and $V_{\text{el,trans}}(\text{Cl}_2\text{S}_2) \approx 5357 \text{ cm}^{-1}$ [4]. Accordingly, extremely small torsional tunneling splittings for the vibrational ground state of $\Delta E_{\pm} = 10^{-12} \text{ hc cm}^{-1}$ [3] for T₂S₂ and $\Delta E_{\pm} = 10^{-76} \text{ hc cm}^{-1}$ [4] for Cl₂S₂ were calculated. For such small tunneling splittings, the special situation may arise that the energy difference between the enantiomers of a chiral molecule ΔE_{pv} , which is caused by the parity-violating electroweak interaction, is larger than the tunneling splitting. Normally, the inclusion of

parity-violating effective potentials in quantum-chemical calculations is not necessary due to their extremely small size (on the order of $10^{-14\pm 3}$ J mol⁻¹ for molecules consisting of the lighter elements). Parity violation in chiral molecules has regained recently considerable attention due to the discovery of values predicted for parity-violating potentials by recent theoretical methods [5–7] that are an order of magnitude larger than those predicted by older theoretical approaches. For Cl₂S₂, for example, we found that $\Delta E_{\text{pv}} = 10^{-12}$ hc cm⁻¹ \gg $\Delta E_{\pm} = 10^{-76}$ hc cm⁻¹ [4] and for T₂S₂ $\Delta E_{\text{pv}} = 10^{-12}$ hc cm⁻¹ $\approx \Delta E_{\pm} = 10^{-12}$ hc cm⁻¹ [3]. Parity violation becomes dynamically dominant and may be spectroscopically observable for Cl₂S₂ [5][8][9]. It should be noted that Cl₂S₂ was the first system where explicit calculations showed that $\Delta E_{\text{pv}} \gg \Delta E_{\pm}$, although such a result is anticipated for all normally stable chiral molecules. On the other hand, for molecules such as D₂S₂, T₂S₂, and perhaps TSOT *etc.*, weaker effects of parity violation might be observable through time-dependent optical activity in tunneling [10].

In contrast to HOOH and HSSH, where numerous high-resolution spectroscopical investigations exist, little is known about HSOH, although it has been postulated in textbooks as the lowest member of the oxo acids of sulfur together with its sulfoxide isomer. Experimental evidence for the existence of HSOH was found in an Ar-matrix experiment, and some of its fundamental vibrations could be assigned [11]. The existence of HSOH in the gas phase has been established in 1994 by *Iraqi* and *Schwarz* [12] by mass spectroscopy. HSOH and related compounds have also been postulated to be of importance in atmospheric chemistry [13][14]. Only recently, a spectroscopic microwave observation of the vibrational ground state was achieved [15]. Therefore, good predictions of the torsional tunneling splittings for torsional excitation with and without excitation of additional vibrations are useful for spectroscopy and reaction kinetics. To our knowledge, such theoretical investigations on HSOH have not been carried out in the past. Only a few theoretical papers have been published, concerning the molecular structure and vibrational frequencies [16], gas-phase acidity, thermochemistry of its radicals, and a study of the potential for internal rotation [17–22]. However, in these investigations, no vibrational tunneling splittings were calculated. For HSOH, in comparison with the similar ‘parent’ molecules H₂O₂ and H₂S₂, intermediate values for tunneling splittings and parity-violating energy differences are expected. Recently, such theoretical investigations were carried out for H₂O₂ [2][6][7] and H₂S₂ [3][23].

The motivation of the present work has, thus, two main origins. First, a study of parity violation and tunneling in HSOH is a natural complement to our earlier extensive studies of the hydrogen peroxide and hydrogen disulfide isotopomers [2–4][6][7][23–25]. Of particular interest is here the scaling behavior of the parity-violating potentials with the nuclear charge of the heavy-atom centers in the molecule. We have previously investigated this in some detail for the symmetrical series HOOH and HSSH [23][25]. One finds here scaling on the order of $Z^{5\pm 1}$, where one must note the ambiguity of the scaling [25]. We have also investigated in some detail theoretically the question of the necessity of having at least two highly charged nuclear centers [7]. It is, thus, natural to address the question of what happens when two highly charged centers exist with significantly different nuclear charges, though, such as in HSOH, which is intermediate between HOOH and HSSH.

The second motivation is to obtain a better understanding of the vibration–rotation–tunneling dynamics for HSOH isotopomers, which are at the center of some current spectroscopic interest [15]. Indeed, after our work had been completed and reported in relation to some spectroscopic work at meetings, of which some printed records exist already [26][27], some preprinted information became available on synthetic and spectroscopic aspects of HSOH [28][29] that complement some of our work, although they do not cover the range of results reported here. The importance of our predictions for spectroscopic investigations and comparison with experimental results on the HSOH isotopomers will be discussed in detail in a separate publication [26].

We present here theoretical results on mode-selective stereomutation dynamics and parity violation in XSOY with Y, X = H, D, T. The torsional tunneling stereomutation dynamics are investigated with the quasi-adiabatic channel quasi-harmonic reaction path Hamiltonian approach [2][30], which treats the torsional motion anharmonically in detail and all the other coordinates as harmonic (but anharmonically coupled to the reaction coordinate). Parity-violating potentials were calculated with our recent multiconfiguration linear response (MC-LR) approach in the random-phase approximation [31]. Our results will be also discussed in relation to the analogous molecules mentioned.

2. Theory and Method of Calculation. – *Fig. 1* shows the calculated C_1 -asymmetrical equilibrium geometry of the stable isomer HSOH.

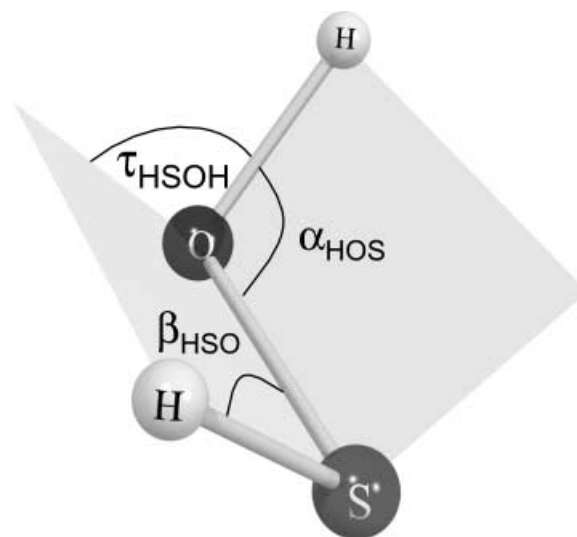


Fig. 1. Chiral, C_1 -asymmetrical equilibrium structure calculated ab initio with MP2/aug-cc-pVTZ. The structural parameters are given in Table 2 (*P*-isomer).

The torsional tunneling dynamics were calculated with the quasi-adiabatic channelreaction path Hamiltonian (RPH) treatment described in detail in [2][3][30]. In brief, it is a modified version of the RPH treatment formulated by

Miller, Handy, and Adams [32]. We introduce the one-dimensional Hamiltonian $\hat{H}_q(\hat{p}, q)$, which depends only upon the reaction coordinate q and its conjugate momentum \hat{p} ,

$$\hat{H}_q = \frac{1}{2}\hat{p}G\hat{p} + u(q) + V_{\text{el}}(q) \quad (1)$$

$u(q)$ is the pseudopotential (see [33]) and V_{el} the *Born–Oppenheimer* potential energy along the minimum-energy path. The momentum operator \hat{p} has its usual definition

$$\hat{p} = -i\hbar \frac{\partial}{\partial q} \quad (2)$$

The effective inverse reduced mass G is obtained by pointwise inversion according to Eqn. 3:

$$G^{-1}(q) = \sum_{i=1}^N \frac{\partial \mathbf{a}_i(q)}{\partial q} \frac{\partial \mathbf{a}_i(q)}{\partial q} \quad (3)$$

with the reference geometry $\mathbf{a}_i(q)$ in terms of the mass-weighted Cartesian coordinate vectors of the atoms i . $u(q)$ is the pseudo-potential. The complete vibrational Hamiltonian is given by

$$\hat{H}(\hat{p}, q, \{\hat{P}_k, Q_k\}) = \hat{H}_Q(\{\hat{P}_k, Q_k\}; q) + \hat{H}_q(\hat{p}, q) \quad (4)$$

where the first part depends on the ‘fast’ $3N - 7$ mass-weighted normal coordinates Q_k and their conjugate momenta \hat{P}_k , and parametrically upon q , the ‘slow’ reaction channel coordinate.

Within the RPH model, we introduce the adiabatic approach for the eigenfunctions of the full hamiltonian \hat{H} :

$$\Psi_m^{(n)}(\vec{Q}, q) = \chi_m^{(n)}(q) \varphi_n(\vec{Q}; q) \quad (5)$$

$$\left(\langle \varphi_n | \hat{H} | \varphi_n \rangle_Q - E_m^{(n)} \right) \chi_m^{(n)}(q) = 0 \quad (6)$$

The semicolon indicates a parametric dependence on q and $\langle \rangle_Q$ the integration over \vec{Q} . In the ‘exact’ adiabatic picture, $\varphi_n(\vec{Q}; q)$ are the eigenfunctions of the Hamiltonian (Eqn. 4) for fixed values of q . Here, they are approximated by a product of one-dimensional harmonic-oscillator eigenfunctions $\psi_{n_k}^{(k)}(Q_k; q)$ so that n becomes a multiindex. Eqn. 6 is solved numerically in a discrete variable representation (DVR).

The reaction path was calculated as a minimum-energy path, with the dihedral or torsion angle $\tau(\text{HSOH})$ as reaction coordinate in steps of 10 degrees (see Fig. 2). This type of reaction path is invariant under isotopic substitution. For each point on the reaction path, the electronic energy, forces, and force constants were calculated with

the Gaussian 94 program package [34]. The electron correlation was treated by second-order *Møller–Plesset* perturbation theory (full MP2), and the standard 6-311 + G*, aug-cc-pVDZ, and aug-cc-pVTZ basis sets were used. The calculations of parity-violating potentials were carried out with the MC-LR approach in the random-phase approximation (RPA), which is described in detail in [31].

The accuracy of the quasiharmonic-quasiadiabatic channel RPH approach was discussed in some detail before [2][3]. We note that predictions for tunneling splittings are expected to be fairly accurate, except for intrinsic *ab initio* error, whereas absolute vibrational–rotational–tunneling energies are less accurate, but are not needed for the present discussions.

3. Results and Discussion. – *Table 1* compares the harmonic wavenumbers for hydrogen thioperoxide calculated *ab initio* on the MP2 level of theory for three different basis sets with a CISD [16] *ab initio* calculation and the experimentally known fundamental wavenumbers determined in an Ar-matrix measurement [11]. In *Table 1*, also the corresponding experimental data for DSOD and the harmonic wavenumbers for a MP2 calculation with the aug-cc-pVTZ standard basis set are given. One finds the typical deviations between the results from experiment and from the *ab initio* calculations. One part of the discrepancy is due to fundamentals being defined differently from harmonic frequencies because of anharmonicity, and another part is due to the typical *ab initio* error in harmonic frequencies. One exception is the OH stretching frequency measured in an Ar-matrix experiment [11], which shows a surprisingly large deviation of more than 10% from the calculated values, and, thus, one might suspect either a strong matrix shift, or the particular experimental assignment to be questionable, because the corresponding OD stretching frequency of DOSD determined in an Ar-matrix experiment shows the more-typical deviation of 4% from the calculated harmonic frequency. However, in [11], a band at 3606 cm^{-1} has been assigned to HOOH, which might be reassigned as the OH-stretching fundamental of HSOH. All in all, the calculations with the aug-cc-pVDZ or the aug-cc-pVTZ basis sets give the best agreement with the experimental data. In *Table 2*, the optimized equilibrium structures are listed for the above-mentioned calculations. *Table 2* also summarizes the calculated *cis* and *trans* barrier heights, $V_{\text{el},\text{trans}}$ and $V_{\text{el},\text{cis}}$ (with $V_{\text{el},\text{trans}} = V(\tau = 180^\circ) - V(\tau_{\text{min}})$ and $V_{\text{el},\text{cis}} = V(\tau = 180^\circ) - V(\tau_{\text{min}})$), of the torsional electronic potential energy. The calculation on the MP2 level of theory with the aug-cc-pVTZ basis set should be a reasonable compromise taking computational costs in relation to the accuracy of the results into account. The results presented in *Tables 1* and *2* indicate that our largest basis set used (aug-cc-pVTZ) at the MP2 level of theory should be adequate for our investigation, as we aim at a good overall description rather than a precise prediction of a particular experimental result.

In *Table 3*, we give, for reasons of completeness, all harmonic wavenumbers calculated *ab initio* (MP2/aug-cc-pVTZ) for all possible hydrogen isotopomers of HSOH, as well as the corresponding band strengths in terms of the integrated cross sections G_i . The numbering of the fundamentals corresponds to the HSOH fundamentals. The integrated cross sections G_i are calculated in the double-harmonic approximation and are defined through the practical *Eqn. 7* [35]:

Table 1. Calculated Harmonic and Experimental Wavenumbers for the Fundamental Transitions of HSOH and DSOD. For the calculated values, the MP2 level of theory is used if not otherwise indicated. All values are given in cm^{-1} . In the following assignments, s refers to a stretching and b to a bending mode: $\nu_1 = s(\text{OX})$, $\nu_2 = s(\text{SX})$, $\nu_3 = b(\text{XOS})$, $\nu_4 = b(\text{XSO})$, $\nu_5 = s(\text{SO})$, and $\nu_6 = \text{torsion}$, with $X = \text{H, D}$.

	HSOH				DSOD		
	Exper. [11] Ar matrix	6-31 + G*	aug-cc-pVDZ	aug-cc-pVTZ	CISD-DZ + P [16]	Exper. [11]	aug-cc-pVTZ
ν_1	3425.0	3721.1	3774.9	3801.9	4005	2661.0	2769.2
ν_2	–	2740.4	2706.6	2713.9	2770	–	1949.86
ν_3	1177.0	1220.3	1196.0	1197.8	1244	866.3	874.92
ν_4	–	1035.5	997.2	1029.2	1064	–	744.23
ν_5	763.0	763.8	749.3	779.2	808	774.8	788.34
ν_6	448.8	474.8	456.2	472.8	489	331.8	345.46

Table 2. Calculated cis and trans Barrier Heights (electronic potential energies: $V_{\text{el,trans}} = V_{\text{el}}(\tau_{\text{HSOH}} = 180^\circ) - V_{\text{el}}(\tau_{\text{HSOH}} = \text{HSOH min. geo.})$ and $V_{\text{el,cis}} = V_{\text{el}}(\tau_{\text{HSOH}} = 0^\circ) - V_{\text{el}}(\tau_{\text{HSOH}} = \text{HSOH min. geo.})$) and Calculated Equilibrium Geometries of HSOH for Various Basis Sets on the MP2 Level of Theory, if Not Otherwise Indicated

	6-31 + G*	aug-cc-pVDZ	aug-cc-pVTZ	CISD/DZ + P [16]
r_{SO}/pm	170.0	172.0	167.9	168.6
r_{SH}/pm	134.5	135.5	134.2	134.0
r_{OH}/pm	97.6	97.1	96.5	95.9
$\beta_{\text{HSO}}/^\circ$	97.47	97.42	98.12	97.8
$\alpha_{\text{HOS}}/^\circ$	107.47	105.54	106.46	107.6
$\tau_{\text{HSOH}}/^\circ$	94.29	92.52	91.78	92.3
$V_{\text{el,trans}}/\text{cm}^{-1}$	1374.7	1378.2	1473.5	–
$V_{\text{el,cis}}/\text{cm}^{-1}$	2585.0	2108.2	2164.2	–

$$G_i = \frac{8\pi^3}{(4\pi\epsilon_0)(3hc)} |\langle v_i = 1 | \mu | v_i = 0 \rangle|^2 \cong 41.624 \left(\frac{|\langle v_i = 1 | \mu | v_i = 0 \rangle|}{\text{Debye}} \right)^2 \text{pm}^2 \quad (7)$$

G_i is, thus, proportional to the square of the electric dipole transition moment for the fundamental transition in the harmonic approximation for the normal mode ν_i and using the linear approximation for the electric dipole moment along this normal coordinate. Reporting of G_i is preferable over the frequently reported $A_i = \omega_i \cdot N_A \cdot G_i$ because no additional error is introduced in G_i through the usual *ab initio* error in ω_i .

Table 4 summarizes the results for the torsional tunneling splittings $\Delta\tilde{\nu}_i = \tilde{\nu}(A^-) - \tilde{\nu}(A^+)$ of the first six pure torsional states of hydrogen thioperoxide and all its hydrogen isotopomers. As is discussed in [26] in more detail, our RPH result for the vibrational ground state of HSOH of $2.34 \cdot 10^{-3} \text{ cm}^{-1}$ agrees very well with the experimental value, particularly in view of the absence of any adjustment of the present prediction. For the isotopomers of HSOH, no experimental tunneling splittings are known. However, we expect that our data are good estimates and can be used as guidance for future experimental work on HSOH isotopomers.

Table 3. Harmonic Wavenumbers ω_i Calculated ab initio and Band Strengths G_i of XSOY Calculated with the aug-cc-pVTZ Basis Set on the MP2 Level of Theory in the Double-Harmonic Approximation. The values of ω_i are given in cm^{-1} and those of G_i in pm^2 . In the following approximate assignments, s refers to a stretching and b to a bending mode: $\nu_1 = s(\text{OY})$, $\nu_2 = s(\text{SX})$, $\nu_3 = b(\text{YOS})$, $\nu_4 = b(\text{XSO})$, $\nu_5 = s(\text{SO})$, $\nu_6 = \text{torsion}$ where X = H, D, T. In this Table, the numbering of the fundamentals corresponds to the HSOH fundamentals.

	ω_1	ω_2	ω_3	ω_4	ω_5	ω_6
HSOH	3801.94	2713.91	1197.78	1029.23	779.19	472.78
HSOD	2769.40	2713.79	874.97	1028.25	776.91	391.76
HSOT	2326.75	2713.96	732.26	1027.79	778.76	360.69
DSOH	3801.95	1949.87	1197.47	745.85	788.77	435.20
DSOD	2769.23	1949.86	874.92	744.23	786.34	345.46
DSOT	2326.74	1949.85	731.94	743.73	788.39	309.62
TSOH	3801.95	1617.68	1197.40	635.19	782.27	421.94
TSOD	2769.23	1617.67	874.86	633.25	779.88	328.51
TSOT	2326.73	1617.67	732.16	632.39	781.96	290.42
	G_1	G_2	G_3	G_4	G_5	G_6
HSOH	0.386	0.043	0.563	0.033	1.296	2.604
HSOD	0.298	0.048	0.491	0.047	1.181	1.531
HSOT	0.275	0.041	0.069	0.053	1.513	1.180
DSOH	0.387	0.033	0.564	0.300	1.019	3.203
DSOD	0.304	0.033	0.496	0.319	0.904	1.938
DSOT	0.274	0.033	0.103	0.331	1.205	1.448
TSOH	0.387	0.029	0.564	0.042	1.566	4.219
TSOD	0.304	0.029	0.493	0.080	1.149	2.84
TSOT	0.274	0.029	0.063	0.100	1.484	1.648

Table 4. Torsional Tunneling Splittings $\Delta\tilde{\nu}_i = \tilde{\nu}(\text{A}^-) - \tilde{\nu}(\text{A}^+)$ for Pure Torsional States $\tilde{\nu} = \nu_i \cdot \tilde{\nu}_i$ of XSOY (X, Y = H, D, and T; aug-cc-pVTZ basis set). All values are given in cm^{-1} and are calculated within our quasiharmonic quasiadiabatic channel RPH approximation.

ν_i :	$\Delta\tilde{\nu}_i$					
	0	1	2	3	4	5
HSOH	$2.34 \cdot 10^{-3}$	0.147	3.805	42.21	135.2	199.5
HSOD	$1.15 \cdot 10^{-4}$	$9.14 \cdot 10^{-3}$	0.317	5.88	48.32	118.9
HSOT	$2.54 \cdot 10^{-5}$	$2.23 \cdot 10^{-3}$	$8.72 \cdot 10^{-2}$	1.900	21.96	85.82
DSOH	$6.82 \cdot 10^{-4}$	$4.81 \cdot 10^{-2}$	1.429	20.46	96.77	158.6
DSOD	$1.14 \cdot 10^{-5}$	$1.06 \cdot 10^{-3}$	$4.43 \cdot 10^{-2}$	1.429	13.81	68.79
DSOT	$1.16 \cdot 10^{-6}$	$1.23 \cdot 10^{-4}$	$5.94 \cdot 10^{-3}$	0.168	2.93	27.08
TSOH	$4.18 \cdot 10^{-4}$	$3.08 \cdot 10^{-2}$	0.964	14.99	82.71	146.8
TSOD	$4.21 \cdot 10^{-6}$	$4.17 \cdot 10^{-4}$	$1.86 \cdot 10^{-2}$	0.478	7.26	48.53
TSOT	$2.81 \cdot 10^{-7}$	$3.21 \cdot 10^{-5}$	$1.68 \cdot 10^{-3}$	$5.24 \cdot 10^{-2}$	1.04	12.42

Normally, an isotopomer with a higher effective reduced tunneling mass has a longer tunneling time. An about four orders of magnitude increase is predicted here for the stereomutation time $t_s = (2c\Delta\tilde{\nu})^{-1}$ in going from HSOH ($t_s = 7 \cdot 10^{-9}$ s) to TSOT ($t_s = 6 \cdot 10^{-5}$ s) (ground-state values). This behavior is quite similar to that observed for HOOH and HSSH.

A question of considerable general current interest in chemical-reaction dynamics concerns vibrational-mode selectivity [36–38]. As we have discussed for the case of

H₂O₂ [2], hydrogendisulfane H₂S₂ [3], and dichlorodisulfane Cl₂S₂ [4], it is of interest, whether excitation of certain, nontorsional vibrational modes promotes ('catalyzes') or inhibits the stereomutation dynamics. The results of our investigation of the mode selectivity of the tunneling process in hydrogen thioperoxide isotopomers are summarized in *Table 5*. There are no experimental data available for the tunneling splittings in excited vibrational states of the XSOY isotopomers, these are, thus, all *ab initio* predictions. It is predicted that an excitation of ν_1 (s(XO)) or ν_2 (s(XS)) inhibits stereomutation in all isotopomers. ν_3 (b(XOS)) is an inhibiting mode as well except for HSOD, HSOT, and DSOT. The excitation of ν_4 (b(XSO)); with exception of HSOD, HSOT, and DSOT) or ν_5 (s(SO)) or ν_6 (torsion) enhances the stereomutation dynamics, ν_6 , for example, by almost a factor of 100, which is, of course, not unexpected. The overall picture is similar to HSSH [3] and HOOH [2]. For HSSH, the mode-specific effects are generally less pronounced, and the tunneling splittings are much smaller, whereas, in HOOH, more-pronounced mode-specific catalysis and inhibition was found [2].

Table 5. *Mode-Specific Stereomutation Tunneling of XSOY* (X, Y: H, D, and T): *Torsional Tunneling Splittings* $\Delta\tilde{\nu}_i = \tilde{\nu}(A^-) - \tilde{\nu}(A^+)$ for *Fundamental Excitations* ν_i (RPH with aug-cc-pVTZ basis set)

		ν_0	ν_1	ν_2	ν_3	ν_4	ν_5	ν_6
HSOH	$\Delta\tilde{\nu}_i(\text{RPH})/10^{-4}\text{cm}^{-1}$	23.39	21.77	16.72	18.49	29.95	25.53	1473
HSOD	$\Delta\tilde{\nu}_i(\text{RPH})/10^{-4}\text{cm}^{-1}$	1.150	1.053	0.773	1.488	0.868	1.327	91.40
HSOT	$\Delta\tilde{\nu}_i(\text{RPH})/10^{-4}\text{cm}^{-1}$	0.254	0.240	0.161	0.324	0.216	0.270	22.34
DSOH	$\Delta\tilde{\nu}_i(\text{RPH})/10^{-4}\text{cm}^{-1}$	6.821	6.301	5.219	6.347	7.179	7.793	480.8
DSOD	$\Delta\tilde{\nu}_i(\text{RPH})/10^{-4}\text{cm}^{-1}$	0.114	0.106	0.081	0.087	0.150	0.134	10.64
DSOT	$\Delta\tilde{\nu}_i(\text{RPH})/10^{-4}\text{cm}^{-1}$	0.012	0.011	0.008	0.021	0.006	0.015	1.23
TSOH	$\Delta\tilde{\nu}_i(\text{RPH})/10^{-4}\text{cm}^{-1}$	4.181	3.851	3.315	4.012	4.385	4.698	307.9
TSOD	$\Delta\tilde{\nu}_i(\text{RPH})/10^{-4}\text{cm}^{-1}$	0.042	0.039	0.031	0.036	0.050	0.050	4.17
TSOT	$\Delta\tilde{\nu}_i(\text{RPH})/10^{-4}\text{cm}^{-1}$	0.003	0.003	0.002	0.002	0.004	0.003	0.321

Finally, we compare the tunneling splittings with calculations for the parity-violating energy difference ΔE_{pv} , which we take here as the difference of parity-violating potentials (or total energies) at the calculated equilibrium geometries of the enantiomers

$$\Delta E_{\text{pv}} \approx E_{\text{pv}}(P) - E_{\text{pv}}(M) \quad (8)$$

$$\approx 2E_{\text{pv}}(P) \quad (9)$$

Table 6 summarizes the results for ΔE_{pv} for HSOH obtained for different basis sets with the MP2/aug-cc-pVTZ equilibrium structure (see *Table 2*). For the two largest basis sets (aug-cc-pVDZ and aug-cc-pVTZ), the value converges to *ca.* $\Delta E_{\text{pv}} \approx 3.7 \cdot 10^{-13}$ hc cm⁻¹, and this thus seems to be a reasonable estimate of the true value. There is a strong dependence of E_{pv} on the torsional angle (see *Fig. 2*), as in other cases [3][4][7][23][31].

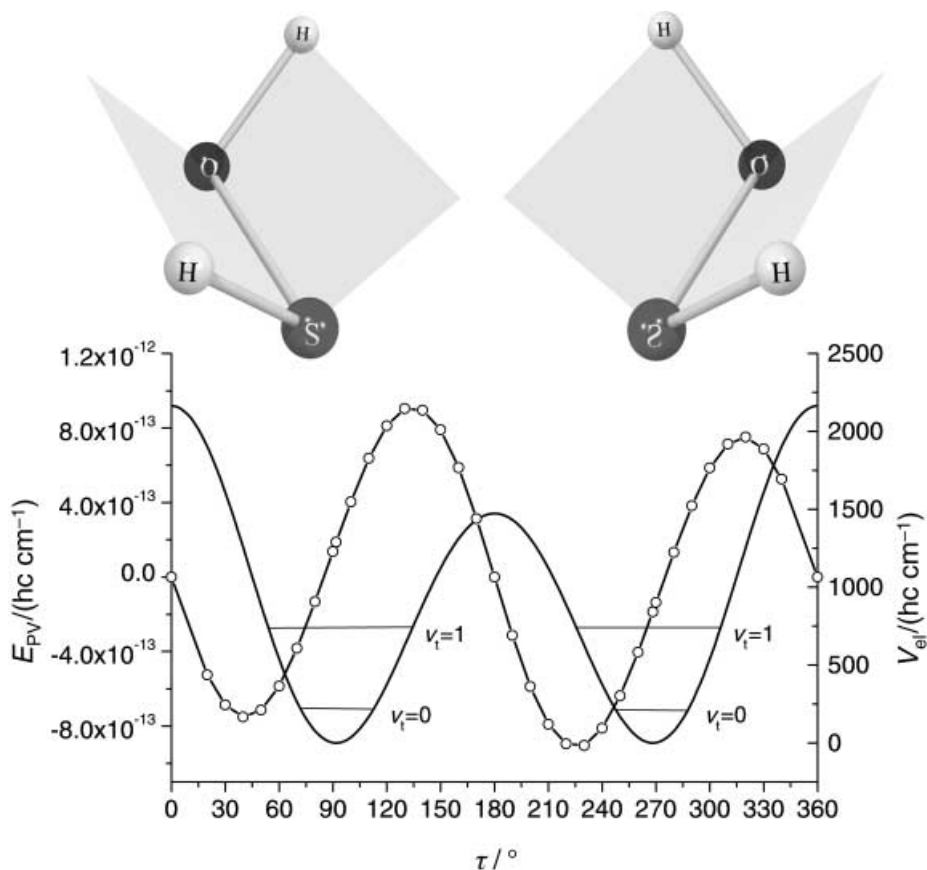


Fig. 2. Parity-conserving electronic torsional potential $V_{el}(\tau)$ (plain full line; MP2/aug-cc-pVTZ) and parity-violating potential $E_{pv}(\tau)$ (circles; RPA/aug-cc-pVTZ). Also indicated are the lower vibrational (torsional) levels.

Table 6. Parity-Violating Energy Difference $\Delta E_{pv} = E_{pv}(P) - E_{pv}(M)$ for HSOH, All Results Employing the MP2/aug-cc-pVTZ Equilibrium Structure Shown in Table 2

	Method	$\Delta E_{pv}/10^{-13} \text{hc} \cdot \text{cm}^{-1}$
HSOH	RPA/6-31G	2.42
	RPA/cc-pVDZ	4.12
	RPA/aug-cc-pVDZ	3.68
	RPA/aug-cc-pVTZ	3.74

In Table 7, we show values for $|\Delta E_{pv}|$ and ΔE_{\pm} for a series of dichalcogenides. The roughly rounded values for ΔE_{\pm} are for the vibrational ground state and the ‘current best estimate’ for $|\Delta E_{pv}|$. Due to the low electroweak charges of the hydrogen isotope nuclei compared to oxygen and sulfur [7][31], the values for ΔE_{pv} for different isotomers are practically identical.

Table 7. Comparison of Theoretically Calculated $|\Delta E_{pv}|$ and $|\Delta E_{\pm}|$ for Various Molecules. Values for δE_{pv} are calculated at the equilibrium structures without vibrational corrections.

Molecule	$ \Delta E_{pv} /hc \cdot \text{cm}^{-1}$	$ \Delta E_{\pm} /hc \cdot \text{cm}^{-1}$	Ref.
H ₂ O ₂	$4 \cdot 10^{-14}$	11	[2][31][39]
D ₂ O ₂	$4 \cdot 10^{-14}$	2	[2][31]
T ₂ O ₂	$4 \cdot 10^{-14}$	0.5	this work
HSOH	$4 \cdot 10^{-13}$	$2 \cdot 10^{-2}$	this work
DSOD	$4 \cdot 10^{-13}$	$1 \cdot 10^{-5}$	this work
TSOT	$4 \cdot 10^{-13}$	$3 \cdot 10^{-7}$	this work
H ₂ S ₂	$1 \cdot 10^{-12}$	$2 \cdot 10^{-6}$	[3]
D ₂ S ₂	$1 \cdot 10^{-12}$	$5 \cdot 10^{-10}$	[3]
T ₂ S ₂	$1 \cdot 10^{-12}$	$1 \cdot 10^{-12}$	[3]
Cl ₂ S ₂	$1 \cdot 10^{-12}$	$\approx 10^{-76a}$	[4]

^a) Extrapolated value.

4. Conclusions and Outlook. – The question on the scaling of the parity-violating potentials addressed in the *Introduction* can be answered approximately from the results presented in *Tables 6* and *7*. Clearly, the parity-violation energy differences ΔE_{pv} between enantiomers of HSOH are intermediate between the values for HOOH and HSSH, closer to those of HSSH. We resist the temptation to make a more-quantitative statement or to generalize this rule too widely. In view of the discussion presented in some detail in [25], no really simple scaling law is expected for the ΔE_{pv} at the equilibrium geometries (or in the ground state, if stabilized by large ΔE_{pv} [5][8]). One important reason for this lack of simple scaling can be understood from the strong conformational dependence of E_{pv} illustrated in *Fig. 2*. Indeed, the maximum value of ΔE_{pv} as a function of conformation shown in this figure for HSOH would be *ca.* $2 \times 10^{-12} \text{ cm}^{-1}$, five times larger than the value for the equilibrium geometry, and qualitatively similar – but not identical – observations can be made for H₂O₂ and H₂S₂ (maximum ΔE_{pv} is *ca.* $8 \times 10^{-12} \text{ cm}^{-1}$ in the latter example as a function of conformation). As we have discussed several times before, it is the subtle interplay between electroweak charges, nuclear charges, and resulting electronic structures and wavefunctions, and finally the conformational and structural dependence of ΔE_{pv} that determines the potentially observable [5][8] parity-violating energy differences in chiral molecules.

For all H₂O₂ isotopomers, the tunneling splittings are much larger than the parity-violating potentials. This means that their observable energy eigenstates can be considered to have well-defined parity (and no well-defined chirality) [3][5][9]. The average mixing of the opposite parity, due to the parity-violating energy difference, into these ‘pure parity’ levels is on the order of $x = (|\Delta E_{pv}|/|\Delta E_{pv}|)^2 \approx 10^{-28}$ in this case, which will hardly be detectable by any of the currently available or proposed spectroscopic techniques. The situation is quite similar for HSOH and its isotopomers, and for H₂S₂ ($x \approx 10^{-13}$). For D₂S₂, a mixing of $x \approx 10^{-6}$ is estimated (and even more for some excited vibrational levels). Although the levels have also in these cases essentially pure parity (and no chirality), the mixing of the opposite parity could perhaps be just

detectable with advanced spectroscopic techniques. For T_2S_2 , $|\Delta E_{pv}|$ and $|\Delta E_{\pm}|$ are almost equal, and here the mixing of levels of different parity is, therefore, pronounced. T_2S_2 was the first molecule for which such mixing has been explored by quantitative theory. In principle, such a case could be investigated by the study of time-dependent optical activity [10] although ΔE_{pv} is not a directly measurable quantity in these situations. For Cl_2S_2 , the situation is completely reversed, since $|\Delta E_{pv}|$ is much larger than $|\Delta E_{\pm}|$. In this case, the molecular eigenfunctions are localized with well-defined handedness ('right' and 'left'), and the dynamics of chirality is dominated by parity violation. This type of situation prevails for ordinary stable chiral molecules, and here $|\Delta E_{pv}|$ can be measured by the technique proposed in [8].

The quasi-adiabatic channel quasi-harmonic reaction path Hamiltonian approach [2] allows us to make quantitative *ab initio* predictions of good accuracy for the stereomutation tunneling splittings of the series of chalcogene derivatives of the HOOH family, which are chiral in their equilibrium geometries. The stereomutation process in these compounds is dominated by the torsional motion, and the theoretical approach treats the problem in all six internal degrees of freedom, where the influence of the nontorsional vibrational modes is taken into account approximately. This allows us to demonstrate mode-selective catalysis and inhibition of stereomutation by the various vibrational modes in XSOY (X, Y = H, D, T). The only available experimental tunneling splitting of the vibrational ground state agrees well with our theoretical result [26]. Our work provides theoretical predictions for tunneling splittings of several vibrational and torsional levels of various isotopomers, which may guide the assignment of experimental spectra in the future.

Our work is supported financially by the ETH-Zürich and the *Swiss National Science Foundation*. We enjoyed discussion and correspondence in this investigation with *Gisbert Winnewisser, Helmut Schwarz*, and *H. F. Schaefer III*, as well as help from *Robert Berger, Michael Gottselig, David Luckhaus, Achim Sieben*, and *Jürgen Stohner*. We acknowledge also some recent correspondence with *Jürgen Gauss*.

REFERENCES

- [1] J. D. Dunitz, *Angew. Chem., Int. Ed.* **2001**, *40*, 4167.
- [2] B. Fehrensen, D. Luckhaus, M. Quack, *Chem. Phys. Lett.* **1999**, *300*, 312.
- [3] M. Gottselig, M. Quack, J. Stohner, M. Willeke, *Helv. Chim. Acta* **2001**, *84*, 1846.
- [4] R. Berger, M. Gottselig, M. Quack, M. Willeke, *Angew. Chem., Int. Ed.* **2001**, *40*, 4195.
- [5] M. Quack, *Angew. Chem., Int. Ed.* **1989**, *28*, 571; M. Quack, *Angew. Chem., Int. Ed.* **2002**, *41*, 4618.
- [6] A. Bakasov, T. K. Ha, M. Quack, in 'Proceedings of the 4th Trieste Conference (1995), Chemical Evolution: Physics of the Origin and Evolution of Life', Eds. J. Chela-Flores and F. Rolin, Kluwer Academic Publishers, Dordrecht, 1996, pp. 287–296.
- [7] A. Bakasov, T. K. Ha, M. Quack, *J. Chem. Phys.* **1998**, *109*, 7263.
- [8] M. Quack, *Chem. Phys. Lett.* **1986**, *132*, 147.
- [9] M. Quack, *Nova Acta Leopoldina* **1999**, *NF 81*, 137.
- [10] R. Harris, L. Stodolsky, *Phys. Lett. B* **1978**, *78*, 313.
- [11] R. R. Smardzewski, M. C. Lin, *J. Chem. Phys.* **1976**, *66*, 3197.
- [12] M. Iraqi, H. Schwarz, *Chem. Phys. Lett.* **1994**, *221*, 359.
- [13] N. S. Wang, C. J. Howard, *J. Phys. Chem.* **1990**, *94*, 8787; R. R. Friedl, W. H. Brune, J. G. Anderson, *J. Phys. Chem.* **1985**, *89*, 5505.
- [14] G. S. Tyndal, A. R. Ravishankara, *Int. J. Chem. Kinet.* **1991**, *23*, 483; N. Balucani, L. Beneventi, P. Casavecchia, D. Stranges, G. G. Volpi, *J. Chem. Phys.* **1991**, *94*, 8611.
- [15] G. Winnewisser, personal communication, 2001.

- [16] T. J. Lee, N. C. Handy, J. E. Rice, A. C. Scheiner, H. F. Schaefer III, *J. Chem. Phys.* **1986**, *85*, 3930; H. Wallmeier, W. Kutzelnigg, *J. Am. Chem. Soc.* **1979**, *101*, 2804.
- [17] G. I. Cárdenas-Jirón, A. Toro-Labbé, *J. Mol. Struct.* **1997**, *390*, 79.
- [18] B. T. Luke, A. D. McLean, *J. Phys. Chem.* **1985**, *89*, 4592.
- [19] S. S. Xantheas, T. H. Dunning, *J. Phys. Chem.* **1993**, *97*, 6616.
- [20] R. A. J. O' Hair, C. H. DePuy, V. M. Biermann, *J. Phys. Chem.* **1993**, *97*, 7955.
- [21] A. Goumri, J.-D. R. Rocha, D. Laakso, C. E. Smith, P. Marshall, *J. Chem. Phys.* **1994**, *101*, 9405.
- [22] G. I. Cárdenas-Jirón, J. R. Letelier, T. Toro-Labbé, *J. Phys. Chem. A* **1998**, *102*, 7864.
- [23] A. Bakasov, M. Quack, *Chem. Phys. Lett.* **1999**, *303*, 547.
- [24] B. Kuhn, T. R. Rizzo, D. Luckhaus, M. Quack, M. Suhm, *J. Chem. Phys.* **1999**, *111*, 2565.
- [25] A. Bakasov, R. Berger, T. K. Ha, M. Quack, *Int. J. Quantum Chem.* **2003**, in press.
- [26] M. Quack, M. Willeke, G. Winnewisser, to be published (see also *Chimia*, **2002**, *56*, 381).
- [27] S. Albert, M. Gottselig, M. Hippler, H. Hollenstein, R. Marquardt, L. Oeltjen, M. Quack, H. Schmid, G. Seyfang, A. Sieben, J. Stohner, M. Willeke, 'From Molecules in Motion to Quantum Chemical Kinetics, Laser Chemistry and Molecular Parity Violation', in 'C4 Annual Report 2001/2002', Competence Center for Computational Chemistry, Zurich.
- [28] J. Hahn, M. Behnke, J. Gauss, 'Gas Phase Detection of HSOH (I)', unpublished preprint, 2003.
- [29] G. Winnewisser, F. Lewen, S. Thorwirth, M. Behnke, J. Hahn, J. Gauss, E. Herbst, 'Gas Phase Detection of HSOH (II)', unpublished preprint, 2003.
- [30] B. Fehrensens, D. Luckhaus, M. Quack, *Z. Phys. Chem. N. F.* **1999**, *209*, 1.
- [31] R. Berger, M. Quack, *J. Chem. Phys.* **2000**, *112*, 3148.
- [32] W. H. Miller, N. C. Handy, J. E. Adams, *J. Chem. Phys.* **1980**, *72*, 99.
- [33] R. Meyer, *J. Chem. Phys.* **1970**, *52*, 2053.
- [34] M. J. Frisch, G. W. Trucks, M. Head-Gordon, P. M. W. Gill, M. W. Wong, J. B. Foresman, B. G. Johnson, H. B. Schlegel, M. A. Robb, E. S. Replogle, R. Gomperts, J. L. Andres, K. Raghavachari, J. S. Binkley, C. Gonzalez, R. L. Martin, D. J. Fox, D. J. Defrees, J. Baker, J. J. P. Stewart, J. A. Pople, Gaussian 94, Revision B.1, *Gaussian, Inc.*, Pittsburgh PA, 1995.
- [35] M. Quack, *Annu. Rev. Phys. Chem.* **1990**, *41*, 839.
- [36] D. W. Lupo, M. Quack, *Chem. Rev.* **1987**, *87*, 181.
- [37] K. von Puttkamer, M. Quack, *Chem. Phys.* **1989**, *139*, 31.
- [38] F. F. Crim, *Annu. Rev. Phys. Chem.* **1993**, *44*, 397.
- [39] W. B. Olson, R. H. Hunt, B. W. Young, A. G. Maki, J. W. J. Brault, *J. Mol. Spectrosc.* **1998**, *128*, 12.

Received April 7, 2003